

SPECTRA OF PERFECT STATE TRANSFER HAMILTONIANS ON FRACTAL-LIKE GRAPHS

GAMAL MOGRABY, MAXIM DEREVYAGIN, GERALD V. DUNNE, AND ALEXANDER TEPLYAEV

ABSTRACT. In this paper we study the spectral features, on fractal-like graphs, of Hamiltonians which exhibit the special property of perfect quantum state transfer: the transmission of quantum states without dissipation. The essential goal is to develop the theoretical framework for understanding the interplay between perfect quantum state transfer, spectral properties, and the geometry of the underlying graph, in order to design novel protocols for applications in quantum information science. We present a new lifting and gluing construction, and use this to prove results concerning an inductive spectral structure, applicable to a wide variety of fractal-like graphs. We illustrate this construction with explicit examples for several classes of diamond graphs.

CONTENTS

1. Introduction	1
2. Perfect quantum state transfer on graphs	2
3. Generic spectral properties of \mathbf{H}	6
3.1. Radial eigenvectors of \mathbf{H}	6
3.2. Lifting-&-Gluing Lemma	8
4. Projective limit constructions	8
4.1. Main Inductive Result	10
5. Two examples	11
5.1. Hambly-Kumagai diamond graphs	12
5.2. Lang-Plaut Diamond graphs	15
6. Further General Geometric Constructions: Two-point self similar graphs	18
Acknowledgments	18
References	18
Appendix A. Hambly-Kumagai diamond graphs: Eigenvalues table for level 3 & 4	21
Appendix B. Lang-Plaut diamond graphs: Eigenvalues table for level 3	22

1. INTRODUCTION

The transfer of a quantum state from one location in a quantum network to another is a fundamental task in quantum information technologies, and such a transfer is called *perfect* if it is realized with probability one, that is, without dissipation. Perfect quantum state transfer (we write shortly PQST) has potential applications to the design of sub-protocols for quantum information and quantum computation [Kay74, CVZ17, KLY17a]. Depending on the application, various quantum systems are employed. Typical designs involve information carriers like photons in optical systems [GKH⁺01], or phonons in ion traps [LDM⁺03, SKHR⁺03]. Other promising devices are spin chains. The study of PQST on spin chains was pioneered by S. Bose [Bos03, Bos07], who considered a $1D$ chain of N qubits coupled by a time-independent Hamiltonian. His work generated intense theoretical interest, in particular in questions concerning how to manipulate and engineer Hamiltonians such that a PQST is achieved. Manufacturing such manipulated Hamiltonians will provide pre-fabricated devices for quantum computer architectures, which takes input in one location and outputs it at another without needing to interact with the device. This approach is robust to noise and

Date: March 22, 2022.

2010 Mathematics Subject Classification. 81Q35, 81P45, 94A40, 05C50, 28A80.

Key words and phrases. Information Theory; Functional Analysis; Spectral Theory; Quantum Physics.

hence much less prone to errors. A number of one dimensional cases, where PQST can be achieved, have been found in some XX chains with inhomogeneous couplings, see [Kay74, Bos07, CDEL04, BB05a, BB05b, KS05, ACNO⁺10, BFF⁺12, God12b, BGS08, God12a, VZ12b, and references therein]. Recently there has been active interest to generalize these results to graphs with potentials and to graphs that are not one dimensional [KLY17a, KLY17b, KMP⁺19, VZ12a]. These works illustrate the fact that PQST is a rare phenomenon, for which the construction of explicit examples remains rather non-trivial. Intending to investigate the rich interplay between quantum state transfer and geometries beyond one-dimensional graphs, we showed in a previous paper [DDMT19] that PQST is possible on the large and diverse class of fractal-type diamond graphs. A significant interest in these graphs lies in the fact that their limit spaces constitute a family of fractals, which present different geometrical properties, including a wide range of Hausdorff and spectral dimensions. These graphs have provided an important collection of structures with interesting physical and mathematical properties and a broad variety of geometries, see [MT95, ADT09, HK10, NT08, AR18, AR19, Tep08, MT03, BCH⁺17]. The structure of these graphs is such that they combine spectral properties of Dyson hierarchical models and transport properties of one dimensional chains. The methods that we use are discretized versions of the methods recently developed in [AR18, AR19] (see also [ARHTT18, ST19]), which provides a construction of Green's functions for diamond fractals.

In this paper, we generalize the construction in [DDMT19] and show that it works for any graph possessing a transversal decomposition (see assumption 2.10). More precisely, on such a graph, a Hamiltonian based on nearest-neighbor coupling and with a certain transversal projective structure (see assumptions 2.7) can be engineered to admit a PQST. For more details, see Theorem 2.12. The primary goal of this paper is to understand the spectrum of such Hamiltonians. Advantageous settings to accomplish this task are projective limit spaces. Analysis on projective limit spaces is an active area of current research [CK13b, CK13a]. Barlow and Evans used projective limits to produce a new class of state spaces for Markov processes [BE04]. The spectra of Laplacians on Barlow-Evans type projective limit spaces were studied in [ST19]. We proceed in this paper in the same spirit but dealing with Hamiltonians instead of Laplacians. To this end, we provide a discretized version of a sequence of projective limit spaces [ST19, Definition 2.1, page 3]. By doing so, we are able to construct a sequence of graphs $\{G_i\}_{i \geq 0}$ and equip each G_i with a Hamiltonian \mathbf{H}_i such that PQST can be achieved (under some additional assumptions). As a main result of this paper, we provide a complete description of the spectrum of \mathbf{H}_i . For the convenience of the reader, we state the main result in the following theorem (see the proof of Theorem 4.9 for further details).

Theorem 1.1. *Given $i \geq 1$, there exists J_0, \dots, J_m a collection of Jacobi matrices of the form 3.2 such that*

$$\sigma(\mathbf{H}_i) = \sigma(\mathbf{J}_0) \cup \sigma(\mathbf{J}_1) \cup \dots \cup \sigma(\mathbf{J}_m).$$

The Jacobi matrices J_0, \dots, J_m are easily determined by the construction scheme that generates G_i from G_0 . As we will see, the Jacobi matrices J_0, \dots, J_m reflect geometrical information of the graph G_i . Moreover, this result provides a straightforward algorithm to determine the spectrum $\sigma(\mathbf{H}_i)$. In section 5, we demonstrate how to apply this result on two models of Diamond-type graphs. These models are a particular case of the Berker lattice construction [BO79] and have been initially the focus of considerable work in statistical mechanics (see, for example [DdI83, LTS83, Col85]).

Our work is part of a long term study of mathematical physics on fractals and self-similar graphs [BCD⁺08a, BCD⁺08b, ADT09, ADT10, ABD⁺12, ACD⁺19, Akk13, Dum12, ARKT16, HM19, MDDT], in which novel features of quantum processes on fractals can be associated with the unusual spectral and geometric properties of fractals compared to regular graphs and smooth manifolds.

The paper is organized as follows. Section 2 deals with the construction of Hamiltonians \mathbf{H} satisfying the assumptions 2.7 on graphs satisfying the assumptions 2.10. Section 3 gives a partial description of the spectrum of the Hamiltonian \mathbf{H} by providing some generic spectral statements. Section 4 defines a discrete version of a projective limit space, on which the main result is stated, Theorem 4.9. Section 5 demonstrates how to apply our main result on two models of Diamond-type graphs. Section 6 discusses the results in further geometrical structures.

2. PERFECT QUANTUM STATE TRANSFER ON GRAPHS

In this section, we extend the study of PQST on diamond fractal graphs [DDMT19] to a more general class of graphs. Let $G = (V(G), E(G))$ be a finite connected graph with a vertex set $V(G)$ and an edge set $E(G)$. We equip G with the geodesic metric $d : V(G) \times V(G) \rightarrow \mathbb{R}$, i.e. for $x, y \in V(G)$, $d(x, y)$ gives the

number of edges in a shortest path connecting x and y . Suppose $A \subset V(G)$ is a non-empty set of vertices. The distance of A to a vertex $x \in V(G)$ is defined as

$$d(x; A) = \min\{d(x, y) : y \in A\}.$$

The following definition generalizes the concept of the intrinsically transversal layers introduced in [DDMT19]. This concept can be found in [HO07, page 76] under the name stratification and plays a crucial role in the quantum decomposition of a graph adjacency matrix.

Definition 2.1. Let $A \subset V(G)$, $A \neq \emptyset$ and $n \in \mathbb{N}$. An n -th transversal layer with respect to A is defined as

$$\Pi_A^{-1}(n) = \{x \in V(G) : d(x; A) = n\},$$

where $\Pi_A : V(G) \rightarrow \mathbb{N}$, $\Pi_A(x) = d(x; A)$. A transversal decomposition of G with respect to A is defined as $V(G) = \bigcup_n \Pi_A^{-1}(n)$. Note that $\Pi_A^{-1}(0) = A$.

A quantum state on G is represented by a complex-valued wave function on the vertices $V(G)$. The following Hilbert space will be used as a domain of the constructed Hamiltonian, which realizes perfect quantum state transfer on G .

Definition 2.2. Given $A \subset V(G)$, $A \neq \emptyset$. The space of quantum states is defined by $L^2(G) = \{\psi \mid \psi : V(G) \rightarrow \mathbb{C}\}$ which is a Hilbert space equipped with the inner product

$$(2.1) \quad \langle \psi | \varphi \rangle_A = \sum_{x \in V} \psi(x) \overline{\varphi(x)} \mu_A(x),$$

where the weights are given by $\mu_A(x) = \frac{1}{|\Pi_A^{-1}(n)|}$ for $n = \Pi_A(x)$ and $|\Pi_A^{-1}(n)|$ denotes the number of vertices in the transversal layer $\Pi_A^{-1}(n)$ that contains x .

Another item we consider is the subspace of radial functions. We call a wave function radial with respect to A if its values depend only on the distance from A .

Definition 2.3. Let $V(G) = \bigcup_{n=0}^N \Pi_A^{-1}(n)$ be a transversal decomposition of G with respect to A , for some $A \subset V(G)$, $A \neq \emptyset$. The subspace of radial functions with respect to A is defined by

$$L_{rad}^2(G) = \{\psi \in L^2(G) \mid \psi(x) = \psi(y) \text{ if } \Pi_A(x) = \Pi_A(y)\}.$$

The projection of $L^2(G)$ onto $L_{rad}^2(G)$ is denoted by $Proj : L^2(G) \rightarrow L_{rad}^2(G)$.

The advantage of the transversal decomposition $V(G) = \bigcup_{n=0}^N \Pi_A^{-1}(n)$ is that it induces an auxiliary 1D chain (path graph) $D_N = (V(D_N), E(D_N))$ with a set of vertices $V(D_N) = \{0, \dots, N\}$ and a set of edges $E(D_N) = \{(n-1, n) : 1 \leq n \leq N\}$. A transversal layer $\Pi_A^{-1}(n)$ is identified with the vertex n in the sense that the vertices $n-1$ and n are defined to be adjacent in the 1D chain if and only if their corresponding transversal layers are adjacent. To reduce the perfect quantum state transfer problem from the graph G to the auxiliary 1D chain D_N , we introduce the following Hilbert space $L^2(D_N) = \{\psi \mid \psi : V(D_N) \rightarrow \mathbb{C}\}$ equipped with the standard inner product

$$(2.2) \quad \langle \psi | \varphi \rangle = \sum_{n=0}^N \psi(n) \overline{\varphi(n)}.$$

Moreover we project a wave function in $L^2(G)$ to a wave function in $L^2(D_N)$ through averaging its values on the transversal layers,

$$P : L^2(G) \rightarrow L^2(D_N), \quad \psi \mapsto P\psi(n) = \frac{1}{|\Pi_A^{-1}(n)|} \sum_{x \in \Pi_A^{-1}(n)} \psi(x).$$

Lemma 2.4. Let P^* be the adjoint operator of P , i.e. $\langle P\psi | \varphi \rangle = \langle \psi | P^*\varphi \rangle_A$ for $\psi \in L^2(G)$ and $\varphi \in L^2(D_N)$. Then P^* is given by

$$P^* : L^2(D_N) \rightarrow L^2(G), \quad \varphi \mapsto P^*\varphi(x) = \varphi(\Pi_A(x)).$$

Proof. A simple calculation shows that,

$$\langle P\psi|\varphi\rangle = \sum_{n=0}^N P\psi(n)\overline{\varphi(n)} = \sum_{x \in V} \psi(x)\overline{\varphi(\Pi_A(x))}\mu_A(x) = \langle \psi|P^*\varphi\rangle_A.$$

□

We will use the following lemma later.

Lemma 2.5. *Let $Id_{D_N} : L^2(D_N) \rightarrow L^2(D_N)$ be the identity operator on $L^2(D_N)$. Then*

- (1) *The range of P^* is $L_{rad}^2(G)$.*
- (2) *$Ker P = (L_{rad}^2(G))^\perp$.*
- (3) *$PP^* = Id_{D_N}$.*
- (4) *$P^*P = Proj$.*

Proof. (1) and (3) follow by definition. (2) Use $Ker P = (Range P^*)^\perp$. (4) Decompose $\psi = Proj \psi + \psi_{rad}^\perp$, i.e. $Proj \psi \in L_{rad}^2(G)$ and $\psi_{rad}^\perp \in (L_{rad}^2(G))^\perp$. By (2) it follows $P^*P\psi = P^*P Proj \psi = Proj \psi$, where the last equality holds by the definitions of P and P^* . □

The following mappings are very useful.

Definition 2.6. Let $V(G) = \Pi_A^{-1}(0) \cup \Pi_A^{-1}(1) \dots \cup \Pi_A^{-1}(N)$ be a transversal decomposition of G with respect to A , for some $A \subset V(G)$, $A \neq \emptyset$ and $N \in \mathbb{N}$. We define the following mappings:

- (1) The left-hand side degree of a vertex \mathbf{deg}_- :

$$\mathbf{deg}_- : \Pi_A^{-1}(1) \dots \cup \Pi_A^{-1}(N) \rightarrow \mathbb{N}.$$

Let $x \in \Pi_A^{-1}(n)$ for some $n \in \{1, \dots, N\}$. The mapping $\mathbf{deg}_-(x)$ assigns the vertex x the number of edges that connect x to vertices in $\Pi_A^{-1}(n-1)$.

- (2) The right-hand side degree of a vertex \mathbf{deg}_+ :

$$\mathbf{deg}_+ : \Pi_A^{-1}(0) \dots \cup \Pi_A^{-1}(N-1) \rightarrow \mathbb{N}.$$

Let $x \in \Pi_A^{-1}(n)$ for some $n \in \{0, \dots, N-1\}$. The mapping $\mathbf{deg}_+(x)$ assigns the vertex x the number of edges that connect x to vertices in $\Pi_A^{-1}(n+1)$.

- (3) The same transversal layer degree of a vertex \mathbf{deg}_0 :

$$\mathbf{deg}_0 : \Pi_A^{-1}(0) \dots \cup \Pi_A^{-1}(N) \rightarrow \mathbb{N}.$$

Let $x \in \Pi_A^{-1}(n)$ for some $n \in \{0, \dots, N\}$. The mapping $\mathbf{deg}_0(x)$ assigns the vertex x the number of edges that connect x to vertices in the same transversal layer $\Pi_A^{-1}(n)$.

A Hamiltonian on G is a self-adjoint operator \mathbf{H} acting on $L^2(G)$. It was observed in [DDMT19] that constructing a Hamiltonian, which is not only adapted to the graph structure but also to the given transversal decomposition of the diamond-type graphs, leads indeed to a Hamiltonian, that realizes a perfect quantum state transfer. Motivated by these observations, we impose the following assumptions on \mathbf{H} :

Assumption 2.7 (Assumptions on the Hamiltonian). *The self-adjoint operator \mathbf{H} acting on $L^2(G)$ is assumed to satisfy the following properties:*

- (1) *Nearest-neighbor coupling: for $x, y \in V(G)$, let $\langle x|\mathbf{H}|y\rangle_A = 0$ if x and y are not connected by an edge, i.e., the transition matrix element from the quantum state $|y\rangle$ to $|x\rangle$ is zero if the vertices y and x are not adjacent in G .*
- (2) *Radial coupling: for $x_1, y_1, x_2, y_2 \in V(G)$ such that both x_1, y_1 and x_2, y_2 are adjacent, we set*

$$\begin{aligned} \langle x_1|\mathbf{H}|y_1\rangle_A &= \langle x_2|\mathbf{H}|y_2\rangle_A \\ \text{if } \Pi_A(x_1) &= \Pi_A(x_2) \text{ and } \Pi_A(y_1) = \Pi_A(y_2), \end{aligned}$$

i.e., the transition matrix elements are compatible with the transversal decomposition of F .

- (3) *For $x, y \in \Pi_A^{-1}(n)$, $n \in \{0, \dots, N\}$ we assume $\langle x|\mathbf{H}|x\rangle_A = \langle y|\mathbf{H}|y\rangle_A$. Moreover, if $x, y \in \Pi_A^{-1}(n)$ are adjacent, then we assume $\langle x|\mathbf{H}|y\rangle_A = \langle x|\mathbf{H}|x\rangle_A$.*

Remark 2.8. For a vertex $x \in V(G)$, the quantum state $|x\rangle$ corresponds to the one-excitation state at the vertex x , i.e.

$$|x\rangle = \begin{cases} 1 & \text{on vertex } x \\ 0 & \text{on } V(G) \setminus \{x\}. \end{cases}$$

A Hamiltonian \mathbf{H} on G is related to an operator on the 1D chain D_N by

$$(2.3) \quad \mathbf{J} = P \mathbf{H} P^*,$$

which acts on $L^2(D_N)$. Similarly, we denote the one-excitation states in $L^2(D_N)$ by $|n\rangle = (0, \dots, 1, \dots, 0)$ where the 1 occupies the n -th position. The following proposition gives a simple criterion for determining whether the constructed Hamiltonian \mathbf{H} is self-adjoint or not.

Proposition 2.9. *Let $V(G) = \bigcup_{n=0}^N \Pi_A^{-1}(n)$ be a transversal decomposition of G with respect to A , for some $A \subset V(G)$, $A \neq \emptyset$ and let assumptions 2.7 hold. Then, the Hamiltonian \mathbf{H} is self-adjoint with respect to the inner product 2.1 if and only if \mathbf{J} is self-adjoint with respect to the inner product 2.2.*

Proof. Note that equation (2.3) implies that \mathbf{J} satisfies the nearest-neighbor coupling condition. Hence it is sufficient to consider adjacent vertices, $x \in \Pi_A^{-1}(n) = \{x_1, \dots, x_k\}$ and $y \in \Pi_A^{-1}(n+1) = \{y_1, \dots, y_m\}$ for some $n \in \{0, \dots, N-1\}$. We observe

$$\begin{aligned} \langle n | \mathbf{J} | n+1 \rangle &= (\langle x_1 | + \dots + \langle x_k |) (|\mathbf{H} y_1\rangle + \dots + |\mathbf{H} y_m\rangle) \\ &= \sum_{x_i \in \Pi_A^{-1}(n)} \deg_+(x_i) \langle x | \mathbf{H} y \rangle_A, \end{aligned}$$

where the second equality holds by the radial coupling assumption. Similarly,

$$\langle \mathbf{J} n | n+1 \rangle = \sum_{y_i \in \Pi_A^{-1}(n+1)} \deg_-(y_i) \langle \mathbf{H} x | y \rangle_A.$$

The proposition statement follows as the matching identity $\sum_{x_i \in \Pi_A^{-1}(n)} \deg_+(x_i) = \sum_{y_i \in \Pi_A^{-1}(n+1)} \deg_-(y_i)$ holds. It gives, in fact, the number of edges between the transversal layers $\Pi_A^{-1}(n)$ and $\Pi_A^{-1}(n+1)$. We consider now the diagonal elements

$$\begin{aligned} \langle n | \mathbf{J} n \rangle &= (\langle x_1 | + \dots + \langle x_k |) (|\mathbf{H} x_1\rangle + \dots + |\mathbf{H} x_m\rangle) \\ &= \sum_{x_i \in \Pi_A^{-1}(n)} (\deg_0(x_i) + 1) \langle x | \mathbf{H} x \rangle_A. \end{aligned}$$

Similarly, we have $\langle \mathbf{J} n | n \rangle = \sum_{x_i \in \Pi_A^{-1}(n)} (\deg_0(x_i) + 1) \langle \mathbf{H} x | x \rangle_A$. □

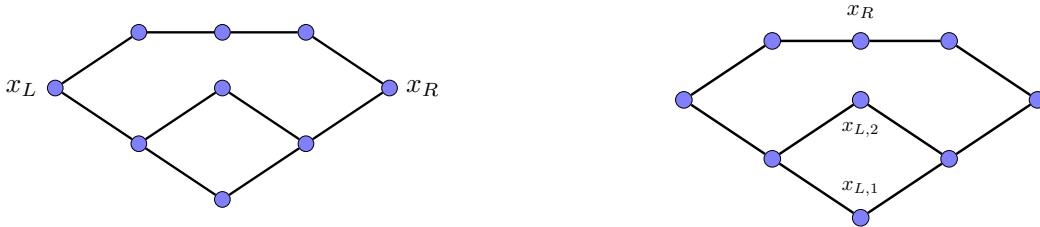


FIGURE 1. (Left) This graph doesn't satisfy the graph assumptions 2.10 with respect to $A = \{x_L\}$. However, it is possible to construct a Hamiltonian that admits PQST from $A = \{x_L\}$ to $B = \{x_R\}$. (Right) The same graph satisfies the graph assumptions 2.10 with respect to $A = \{x_{L,1}, x_{L,2}\}$. Theorem 2.12 implies the possibility of constructing a Hamiltonian that admits PQST from $A = \{x_{L,1}, x_{L,2}\}$ to $B = \{x_R\}$.

From now on, we require that the graph G satisfies the following assumption.

Assumption 2.10 (Assumptions on the graph G). *Let G be a finite connected graph. We assume there exists $A \subset V(G)$, $A \neq \emptyset$ that transversally decomposes $V(G) = \bigcup_{n=0}^N \Pi_A^{-1}(n)$ in such a way that the following holds:*

- (1) *The mappings \deg_+ , \deg_- and \deg_0 are constant on a transversal layer, i.e., for $x, y \in \Pi_A^{-1}(n)$ we have*

$$\deg_+(x) = \deg_+(y), \quad \deg_-(x) = \deg_-(y), \quad \deg_0(x) = \deg_0(y).$$

The following lemma follows in exactly the same way as [DDMT19, Lemma 2, page 8].

Lemma 2.11. *Under the assumptions 2.7 and 2.10, we can prove that the subspace $L_{rad}^2(G)$ is invariant under \mathbf{H} .*

Recall that our primary motivation is to understand how quantum systems in geometries beyond a 1D chain can be engineered to produce sub-protocols of perfect quantum state transfer. Let G be a graph transversally decomposed with respect to A , satisfying the assumptions 2.10 and associated with the 1D chain D_N . We set $A = \{x_{L,1}, \dots, x_{L,m}\}$ and define the quantum state $|A\rangle = |x_{L,1}\rangle + \dots |x_{L,m}\rangle$. Note that $|A\rangle = P^*|0\rangle \in L_{rad}^2(G)$. Similarly, we define the quantum state $|B\rangle = P^*|N\rangle \in L_{rad}^2(G)$. The following theorem provides a sufficient condition of how to design a Hamiltonian on G that achieves a perfect transfer of the quantum state $|A\rangle$ into $|B\rangle$.

Theorem 2.12. *Under the assumptions 2.7 and 2.10, if a PQST on the 1D chain D_N is achieved, i.e., there exists $T > 0$ such that $e^{iT\mathbf{J}}|0\rangle = e^{i\phi}|N\rangle$ for some phase ϕ , then a PQST on G is also achieved with the same time T and phase ϕ , i.e.,*

$$e^{iT\mathbf{H}}|A\rangle = e^{i\phi}|B\rangle \quad \text{and} \quad e^{iT\mathbf{H}}|B\rangle = e^{i\phi}|A\rangle.$$

Proof. In the same way as [DDMT19, Proof of Theorem 1, page 9], we show $e^{iT\mathbf{H}\mathbf{Proj}}|A\rangle - e^{i\phi}|B\rangle \in \text{Ker}(P)$. Using $|A\rangle, |B\rangle \in L_{rad}^2(G)$ we conclude with Lemma 2.11, $e^{iT\mathbf{H}\mathbf{Proj}}|A\rangle = e^{i\phi}|B\rangle$. Let \mathbf{Proj}^\perp be the projection of $L^2(G)$ onto $(L_{rad}^2(G))^\perp$. The statement follows by $(\mathbf{H}\mathbf{Proj} + \mathbf{H}\mathbf{Proj}^\perp)|A\rangle = \mathbf{H}\mathbf{Proj}|A\rangle$ \square

Remark 2.13. In a previous paper [DDMT19], we considered the PQST from an excited state on a single vertex x_L to another excited state on a single vertex x_R . Theorem 2.12 covers additional situations, in which a PQST is achieved between the subsets $A, B \subset V(G)$, where A and B may contain more than a single vertex, see Figure 1 (right). On the other hand, Figure 1 (left) shows an example of a graph that doesn't satisfy the assumptions 2.10 with respect to $A = \{x_L\}$. However, it is possible to construct a Hamiltonian that admits a PQST from $A = \{x_L\}$ to $B = \{x_R\}$.

Let $(H(x, y))_{x, y \in V(G)}$ be the matrix representation of \mathbf{H} with respect to the canonical basis $\{|x\rangle\}_{x \in V(G)}$. The following result relates the matrix elements of \mathbf{H} to \mathbf{J} and can be proved similarly to Proposition 1 in [DDMT19].

Proposition 2.14. *Let $x, y \in V(G)$,*

- (1) $H(x, x) = \frac{1}{\deg_0(x) + 1} \langle \Pi_A(x) | \mathbf{J} | \Pi_A(x) \rangle$.
(2) *Let y be adjacent to x and $\Pi_A(y) = \Pi_A(x) \pm 1$, then $H(x, y) = \frac{1}{\deg_\pm(x)} \langle \Pi_A(x) | \mathbf{J} | \Pi_A(x) \pm 1 \rangle$.*

3. GENERIC SPECTRAL PROPERTIES OF \mathbf{H}

3.1. Radial eigenvectors of \mathbf{H} . The goal in this section is to give a partial description of the spectrum of a Hamiltonian \mathbf{H} satisfying the assumptions 2.7. This part of the spectrum is related to the transversal decomposition of G and consequently can be described for a generic G satisfying the assumptions 2.10. The following lemmas reveal some advantages for considering the induced 1D chain and the Jacobi matrix \mathbf{J} while investigating the Hamiltonian \mathbf{H} . In section 4.1, we will see that this approach is very fruitful. In fact, we will develop this approach further to give a complete description of the spectrum $\sigma(\mathbf{H})$ on a broad class of graphs.

Lemma 3.1. *Let $\mathbf{J} = P\mathbf{H}P^*$, then $\sigma(\mathbf{J}) \subset \sigma(\mathbf{H})$. Moreover, if $\lambda \in \sigma(\mathbf{J})$ is an eigenvalue with the eigenvector v_λ , then P^*v_λ is a corresponding \mathbf{H} -eigenvector.*

Proof. Let $\lambda \in \sigma(\mathbf{J})$ be an eigenvalue corresponding to the eigenvector $v_\lambda \in L^2(D_N)$. Then

$$\lambda P^* v_\lambda = P^* \mathbf{J} v_\lambda = P^* P \mathbf{H} P^* v_\lambda = \text{Proj } \mathbf{H} P^* v_\lambda = \mathbf{H} P^* v_\lambda,$$

where the last equality holds as $\mathbf{H} P^* v_\lambda \in L_{rad}^2(G)$. \square

Note that $P^* v_\lambda \in L_{rad}^2(G)$ and hence we denote it as a radial eigenvector.

Lemma 3.2. *Let $z \notin \sigma(\mathbf{H})$. Then the resolvent operators satisfy $(\mathbf{J} - z)^{-1} = P(\mathbf{H} - z)^{-1} P^*$.*

Proof. Note $z \notin \sigma(\mathbf{H})$ implies $z \notin \sigma(\mathbf{J})$ by Lemma 3.1. We prove that $P(\mathbf{H} - z)^{-1} P^*$ is the inverse operator of $\mathbf{J} - z$. We have

$$\begin{aligned} (\mathbf{J} - z)P(\mathbf{H} - z)^{-1} P^* &= P(\mathbf{H} - z)P^* P(\mathbf{H} - z)^{-1} P^* \\ &= P(\mathbf{H} - z) \text{Proj}(\mathbf{H} - z)^{-1} P^* \\ &= Id_{D_N} \end{aligned}$$

where the equalities hold by Lemmas 2.5 and 2.11. A similar argument shows that $P(\mathbf{H} - z)^{-1} P^*$ is also a left inverse of $\mathbf{J} - z$. \square

Let $P_{\mathbf{J},\lambda}$ and $P_{\mathbf{H},\lambda}$ be the eigenprojections corresponding to $\lambda \in \sigma(\mathbf{J})$ and $\lambda \in \sigma(\mathbf{H})$, respectively.

Theorem 3.3. *Let $\lambda \in \sigma(\mathbf{J})$. Then $P_{\mathbf{J},\lambda} = P P_{\mathbf{H},\lambda} P^*$.*

Proof. A spectral representation of the resolvent operators in lemma 3.2 gives

$$(3.1) \quad \sum_{\tilde{\lambda} \in \sigma(\mathbf{J})} \frac{1}{z - \tilde{\lambda}} P_{\mathbf{J},\tilde{\lambda}} = \sum_{\tilde{\lambda} \in \sigma(\mathbf{H})} \frac{1}{z - \tilde{\lambda}} P P_{\mathbf{H},\tilde{\lambda}} P^*$$

Multiplying both sides of equation (3.1) by $z - \lambda$ and subsequently taking the limit $z \rightarrow \lambda$ will give the result. \square

For the rest of the paper, we assume that the auxiliary 1D chain is equipped with the following Jacobi matrix

$$(3.2) \quad \mathbf{J} = \begin{pmatrix} B_1 & J_1 & 0 & & \\ J_1 & B_2 & J_2 & & \\ 0 & J_2 & B_2 & \ddots & \\ & 0 & \ddots & \ddots & J_N \\ & & & J_N & B_{N+1} \end{pmatrix}.$$

where $B_1, \dots, B_{N+1} \in \mathbb{R}$ and $J_i > 0$ for $i \in \{1, \dots, N\}$. Let $\{p_0(z), \dots, p_{N+1}(z)\}$ be monic polynomials defined by the following recurrence relations:

$$(3.3) \quad \begin{cases} p_0(z) = 1, & p_1(z) = z - B_1, \\ p_k(z) = (z - B_k)p_{k-1}(z) - J_{k-1}^2 p_{k-2}(z), & k = 2, 3, \dots, N+1 \end{cases}$$

The following proposition summarizes some useful spectral properties of \mathbf{J} . For details, the reader is referred to [HO07, p. 48].

Proposition 3.4. *Every zero of $p_{N+1}(z)$ is real and simple. Moreover, $\sigma(\mathbf{J}) = \{\lambda \in \mathbb{C} : p_{N+1}(\lambda) = 0\}$. For an eigenvalue $\lambda \in \sigma(\mathbf{J})$, the corresponding eigenvectors is given by*

$$(3.4) \quad v_\lambda = \left(p_0(\lambda), \frac{p_1(\lambda)}{J_1}, \dots, \frac{p_N(\lambda)}{J_1 \cdots J_N} \right)^t$$

Corollary 3.5. *Let $\lambda \in \sigma(\mathbf{J})$. The corresponding \mathbf{H} -eigenvector is given $P^* v_\lambda$, where v_λ is defined in (3.4).*

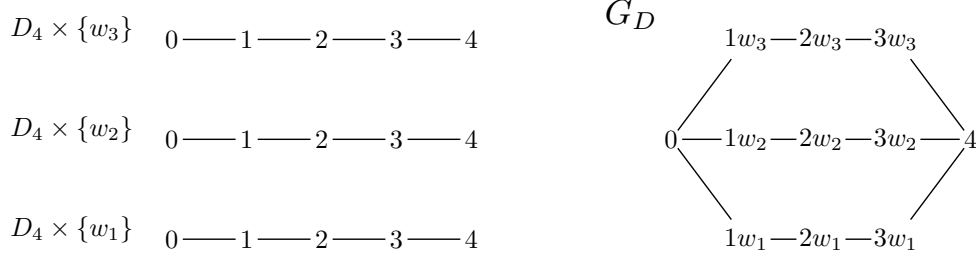


FIGURE 2. (Left) Three copies of the 1D chain D_4 with $V(D_4) = \{0, \dots, 4\}$. The i -th copy is denoted by $D_4 \times \{w_i\}$, where w_i is a letter in the alphabet $W = \{w_1, w_2, w_3\}$. (Right) The graph G_D is constructed by gluing the three copies at the boundary points. Another way of saying this is that the graph G_D is made up of three branches, the w_1 -branch, w_2 -branch and w_3 -branch.

3.2. Lifting-&-Gluing Lemma. This section is devoted to a lemma that will be needed throughout the paper. We consider a 1D chain D_N equipped with a Jacobi matrix \mathbf{J} . When Dirichlet boundary conditions are imposed, we write \mathbf{J}^D for the Jacobi matrix. For a given $k \in \mathbb{N}$, $k \geq 2$ we define G_D to be the graph that is constructed by taking k copies of D_N and gluing their boundary vertices together as shown in Figure 2. To distinguish between the copies, we use the following notation. Given a k -letter alphabet $\{w_1, \dots, w_k\}$, we denote the i -th copy of D_N by $D_N \times \{w_i\}$ and refer to the associated subgraph in G_D as the w_i -branch of G_D . The graph G_D satisfies the assumptions 2.10 with respect to $A = \{0\}$ and D_N is the auxiliary 1D chain. Moreover, the Jacobi matrix \mathbf{J} provides the ingredient needed in Proposition 2.14 to lift and define a Hamiltonian \mathbf{H} on G_D . The following result is very useful.

Lemma 3.6 (Lifting-&-Gluing Lemma). *Let $\lambda \in \sigma(\mathbf{J}^D)$ and v_λ^D be the corresponding \mathbf{J}^D -eigenvector. We define v_λ to be the vector on G_D that coincides with v_λ^D on a w_i -branch and coincides with $-v_\lambda^D$ on another branch, say w_j -branch, for some $j \neq i$, i.e.,*

$$(3.5) \quad v_\lambda = \begin{cases} v_\lambda^D & \text{on the } w_i\text{-branch} \\ -v_\lambda^D & \text{on the } w_j\text{-branch} \\ 0 & \text{elsewhere} \end{cases}$$

Then $\lambda \in \sigma(\mathbf{H})$ and v_λ is a corresponding \mathbf{H} -eigenvector. Moreover, $v_\lambda \in (L_{rad}^2(G_D))^\perp$.

In other words, if we lift a \mathbf{J}^D -eigenvector (Dirichlet eigenvector of \mathbf{J}) to a branch and lift the same vector with the opposite sign to another branch, then assigning zero to the remaining branches and gluing them together, this will result in an eigenvector of \mathbf{H} on G_D with the same eigenvalue. An immediate consequence of Lemma 3.6 is that the spectrum of \mathbf{H} is determined by the spectra of \mathbf{J} and \mathbf{J}^D .

Corollary 3.7. $\sigma(\mathbf{H}) = \sigma(J) \cup \sigma(J^D)$

Proof. The radial eigenvectors are constructed according to Lemma 3.1, which implies $\sigma(J) \subset \sigma(\mathbf{H})$. The remaining eigenvectors are elements of $(L_{rad}^2(G_D))^\perp$ and constructed by the Lifting-&-Gluing Lemma 3.6. Note that for the 1D chain D_N the Jacobi matrices \mathbf{J} and \mathbf{J}^D have $N+1$ and $N-1$ eigenvectors, respectively. Each \mathbf{J} -eigenvector is lifted to a radial \mathbf{H} -eigenvector on G_D and each \mathbf{J}^D -eigenvector generates $k-1$ different \mathbf{H} -eigenvectors on G_D . Note the graph G_D has $(N+1) + (N-1)(k-1)$ vertices. \square

The observation in Corollary 3.7 is the first step in an approach that we will develop further next section. Indeed, we will show that the \mathbf{H} -spectra on a broad class of graphs are determined by the spectra of a collection of Jacobi matrices.

4. PROJECTIVE LIMIT CONSTRUCTIONS

The following definitions are roughly speaking a discrete version of [ST19, Definition 2.1, page 3].

Definition 4.1. Let $k \geq 2$. We refer to a k -letter alphabet $\{w_1, \dots, w_k\}$ as a *vertical multiplier space*. A word of length m is an element of the m -fold product $W^m = W_1 \times \dots \times W_m$, for some vertical multiplier spaces W_1, \dots, W_m . For a word $w \in W^m$, we write shortly $w = w_1 \dots w_m$ instead of $w = (w_1, \dots, w_m)$.

Note that the vertical multiplier spaces W_1, \dots, W_m are not assumed to have the same number of letters.

Definition 4.2. We initialize the graph $G_0 = (V(G_0), E(G_0))$ to be a 1D chain D_N for some $N \geq 1$. We call G_0 the *horizontal base space*.

Remark 4.3. The assumptions on the horizontal base space in [ST19] are very general (local compact second countable Hausdorff space). In this sense, definition 4.2 represents a discretization of a specific case.

Definition 4.4. Given a sequence of vertical multiplier spaces $\{W_i\}_{i \geq 1}$ and a horizontal base space $G_0 = D_N$. We define a sequence of graphs $\{G_i\}_{i \geq 0}$ inductively.

- (1) Suppose $G_{i-1} = (V(G_{i-1}), E(G_{i-1}))$ is given for $i \geq 1$.
- (2) Choose a subgraph $B_i = (V(B_i), E(B_i))$ of G_{i-1} , such that $G_{i-1} \setminus B_i$ is a collection of 1D chains. Note B_i may be an edgeless or a disconnected subgraph.
- (3) For a 1D chain D in $G_{i-1} \setminus B_i$, we set G_D to be the graph that is constructed by taking the copies $D \times \{w_k\}$ for $w_k \in W_i$ and gluing their boundary vertices together as shown in Figure 2.
- (4) We construct G_i by replacing each 1D chain D in $G_{i-1} \setminus B_i$ with the corresponding G_D .

As a convenient notation, we set $V(G_i) = [(V(G_{i-1}) \setminus V(B_i)) \times W_i] \cup V(B_i)$ for the set of vertices of G_i and $E(G_i) = [(E(G_{i-1}) \setminus E(B_i)) \times W_i] \cup E(B_i)$ for the set of edges of G_i , see Figure 3 (Left).

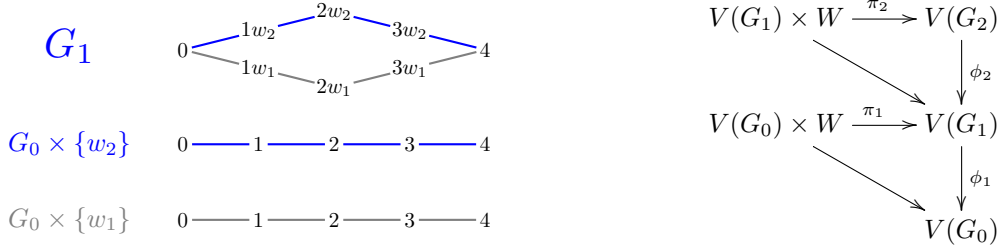


FIGURE 3. (Left) To construct the graph G_1 , we initialize the horizontal base space G_0 to be the 1D chain D_4 with the vertices $\{0, \dots, 4\}$. For the vertical multiplier space, we set $W = \{w_1, w_2\}$. Then G_1 is constructed as in Definition 4.4, where we choose the subgraph B_1 such that $V(B_1) = \{0, 4\}$ and $E(B_1) = \emptyset$. Note that the address assignments of the vertices described in definition 4.4 are shown on the graph of G_1 . (Right) A diagram to display how the different mappings from definition 4.4 are related to each other.

Definition 4.5. Let $\{G_i\}_{i \geq 0}$ be constructed as described in Definition 4.4. We define $\pi_i : V(G_{i-1}) \times W_i \rightarrow V(G_i)$ by

$$\pi_i(x, w) = \begin{cases} (x, w) & \text{if } x \in V(G_{i-1}) \setminus V(B_i) \\ x & \text{if } x \in V(B_i), \end{cases}$$

and the map $\phi_i : V(G_i) \rightarrow V(G_{i-1})$ by

$$\begin{aligned} \phi_i(x, g) &= x & \text{if } x \in V(G_{i-1}) \setminus V(B_i) \\ \phi_i(x) &= x & \text{if } x \in V(B_i). \end{aligned}$$

The following proposition shows that each graph in $\{G_i\}_{i \geq 0}$ admits a natural transversal decomposition, where the horizontal base space G_0 is used as the common auxiliary 1D chain for the entire sequence $\{G_i\}_{i \geq 0}$.

Proposition 4.6. Let $\{G_i\}_{i \geq 0}$ be constructed as described in Definition 4.4. Then for each $i \geq 1$, the graph G_i can be transversally decomposed with respect to $A_i = (\phi_i)^{-1} \circ \dots \circ (\phi_1)^{-1}(0) \subset V(G_i)$. Moreover, for $\Pi_{A_i}(x) = d(x, A_i)$ (see Definition 2.1) we have $\Pi_{A_i}(x) = \phi_1 \circ \dots \circ \phi_i(x)$.

Proof. Note that a vertex in G_i is denoted by $nw_1w_2\dots w_k$, where $n \in \{0, \dots, N\}$ and $w_1w_2\dots w_k \in W^k$. The word $w_1w_2\dots w_k$ can be considered as a vertical coordinate which gives the address of the branch that contains this vertex. On the other hand, the integer n can be considered as a radial coordinate, which gives the distance to $A_i = (\phi_i)^{-1} \circ \dots \circ (\phi_1)^{-1}(0)$. By Definition 4.5 we have $\phi_1 \circ \dots \circ \phi_i(nw_1w_2\dots w_k) = n$ and therefore, this implies $\Pi_{A_i}(x) = \phi_1 \circ \dots \circ \phi_i(x)$. Now G_0 as a 1D chain, it admits a trivial transversal decomposition with respect to $\{0\}$ i.e., $V(G_0) = \Pi_0^{-1}(0) \cup \Pi_0^{-1}(1) \dots \cup \Pi_0^{-1}(N)$, $\Pi_0^{-1}(n) = \{n\}$. Similarly, G_i admits a transversal decomposition with respect to A_i ,

$$V(G_i) = \Pi_{A_i}^{-1}(0) \cup \Pi_{A_i}^{-1}(1) \dots \cup \Pi_{A_i}^{-1}(N),$$

where for $x \in V(G_i)$, we have $x \in \Pi_{A_i}^{-1}(n) \iff \phi_1 \circ \dots \circ \phi_i(x) \in \Pi_0^{-1}(n)$. \square

Each graph in $\{G_i\}_{i \geq 0}$ admits a natural transversal decomposition. One may wonder if these graphs also satisfy the graph assumptions 2.10 with respect to this decomposition. The following example shows that this is not true in general.

Example 4.7. Let the graph \tilde{G}_2 be constructed as described in Figure 4. \tilde{G}_2 does not satisfy the graph assumptions 2.10, as the mappings \deg_+ and \deg_- are NOT constant on the transversal layer $\Pi_0^{-1}(2) = \{2w_2w_2, 2w_1, 2w_2w_1\}$,

$$\begin{aligned} 2 &= \deg_+(2w_1) \neq \deg_+(2w_2w_2) = \deg_+(2w_2w_1) = 1, \\ 2 &= \deg_-(2w_1) \neq \deg_-(2w_2w_2) = \deg_-(2w_2w_1) = 1 \end{aligned}$$

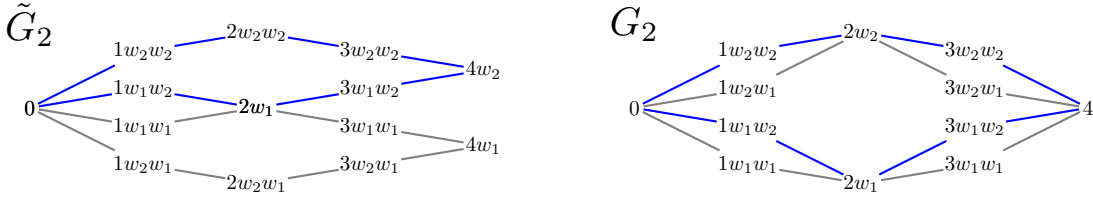


FIGURE 4. The graphs \tilde{G}_2 and G_2 are constructed as described in Definition 4.4. While G_2 satisfies the graph assumptions 2.10, \tilde{G}_2 does not. For the construction of \tilde{G}_2 and G_2 , we set G_1 to be the graph shown in Figure 3. (Left) \tilde{G}_2 is constructed by taking the two copies $G_1 \times \{w_1\}$, $G_1 \times \{w_2\}$ and choosing the subgraph \tilde{B}_2 such that $V(\tilde{B}_2) = \{0, 2w_1\}$ and $E(\tilde{B}_2) = \emptyset$. (Right) G_2 is constructed by taking the two copies $G_1 \times \{w_1\}$, $G_1 \times \{w_2\}$ and choosing the subgraph B_2 such that $V(B_2) = \{0, 2w_1, 2w_2, 4\}$ and $E(B_2) = \emptyset$. Note that G_2 is the level-2 Hambly-Kumagai Diamond graph and denoted by HK_2 . For more details see Section 5.1.

4.1. Main Inductive Result.

- (1) Given a sequence of vertical multiplier spaces $\{W_i\}_{i \geq 1}$ and a 1D chain G_0 .
- (2) Let $\{G_i\}_{i \geq 0}$ and $\{B_i\}_{i \geq 1}$ be constructed as described in Definition 4.4.
- (3) We transversally decompose $\{G_i\}_{i \geq 0}$ as described in Proposition 4.6 and require that each G_i satisfies the graph assumptions 2.10 with respect to this decomposition.

The horizontal base space G_0 plays the role of the auxiliary 1D chain and will be used to lift a Hamiltonian to each G_i , $i \geq 1$. To this end, we equip G_0 with a Jacobi matrix \mathbf{J} of the form (3.2). The Jacobi matrix acts on the Hilbertspace $L^2(G_0) = \{\psi \mid \psi : V(G_0) \rightarrow \mathbb{C}\}$, $\langle \psi \mid \varphi \rangle = \sum_{n=0}^N \psi(n) \overline{\varphi(n)}$. Recall, the transversal decomposition of G_i is with respect to $A_i = (\phi_i)^{-1} \circ \dots \circ (\phi_1)^{-1}(0) \subset V(G_i)$. Hence, we proceed as in Section 2 and equip each G_i with the Hilbert space $L^2(G_i) = \{\psi \mid \psi : V(G_i) \rightarrow \mathbb{C}\}$, $\langle \psi \mid \varphi \rangle_{A_i} = \sum_{x \in V(G_i)} \psi(x) \overline{\varphi(x)} \mu_{A_i}(x)$, where the weights are given by $\mu_{A_i}(x) = 1/|\Pi_{A_i}^{-1}(n)|$ for $n = \Pi_{A_i}(x)$ and $|\Pi_{A_i}^{-1}(n)|$ denotes the number of vertices in the transversal layer $\Pi_{A_i}^{-1}(n)$ that contains x . Another useful item is the pullback operator induced by $\phi_i : V(G_i) \rightarrow V(G_{i-1})$, defined by

$$\phi_i^* : L^2(G_{i-1}) \rightarrow L^2(G_i), \quad \varphi \rightarrow \phi_i^* \varphi(x) = \varphi(\phi_i(x)).$$

The averaging operator and its adjoint are given by

$$\begin{aligned} P_i : L^2(G_i) &\rightarrow L^2(G_0), & \psi &\mapsto P_i \psi(n) = \frac{1}{|\Pi_{A_i}^{-1}(n)|} \sum_{x \in \Pi_{A_i}^{-1}(n)} \psi(x). \\ P_i^* : L^2(G_0) &\rightarrow L^2(G_i), & \varphi &\mapsto P_i^* \varphi(x) = \phi_1^* \dots \phi_i^* \varphi(x) = \varphi(\phi_1 \circ \dots \circ \phi_i(x)). \end{aligned}$$

We are now in a position to construct a Hamiltonian \mathbf{H}_i on G_i , $i \geq 1$:

- (1) Let \mathbf{H}_i be a Hamiltonian on G_i , that satisfies the assumptions 2.7.
- (2) Let \mathbf{H}_i be lifted from G_0 to G_i via, $\mathbf{J} = P_i \mathbf{H}_i P_i^*$.

The following result is a straight forward generalization of Lemma 3.1.

Lemma 4.8. $\sigma(\mathbf{H}_{i-1}) \subset \sigma(\mathbf{H}_i)$. Moreover, if $\lambda \in \sigma(\mathbf{H}_{i-1})$ is an eigenvalue corresponding to the eigenvector v_λ , then $\phi_i^* v_\lambda$ is an \mathbf{H}_i -eigenvector with the same eigenvalue.

The following theorem is our main result and characterizes the spectrum of the Hamiltonian \mathbf{H}_i on G_i , $i \geq 1$.

Theorem 4.9. Given $i \geq 0$, there exists J_0, \dots, J_m a collection of submatrices of \mathbf{J} such that

$$\sigma(\mathbf{H}_i) = \sigma(\mathbf{J}_0) \cup \sigma(\mathbf{J}_1) \cup \dots \cup \sigma(\mathbf{J}_m)$$

Proof. Assume that the statement is correct for $\sigma(\mathbf{H}_{i-1})$. By definition G_i is constructed by replacing each 1D chain in $G_{i-1} \setminus B_i$ with multiple copies glued together at their boundary vertices. Let $\mathbf{J}_0, \dots, \mathbf{J}_k$ be the collection of the Jacobi matrices associated with the 1D chains in $G_{i-1} \setminus B_i$. Using Lemma 4.8 combined with Lemma 3.6 (Lifting-&-Gluing Lemma), we imply $\sigma(\mathbf{H}_i) = \sigma(\mathbf{J}_0) \cup \sigma(\mathbf{J}_1) \cup \dots \cup \sigma(\mathbf{J}_k) \cup \sigma(\mathbf{H}_{i-1})$. \square

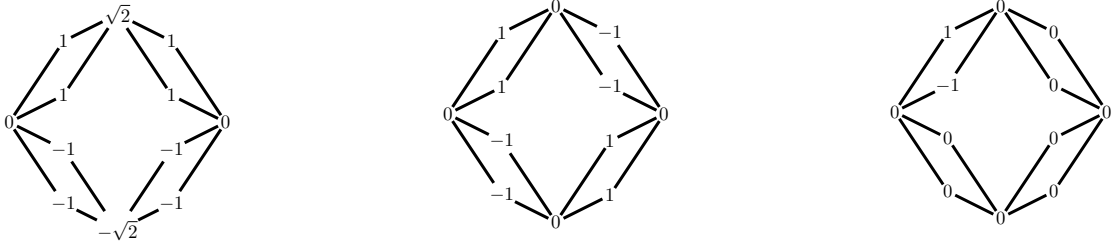


FIGURE 5. Hambly-Kumagai diamond graphs level 2 : (Left) \mathbf{H}_2 -eigenvector for the eigenvalue $\sqrt{3}$. (Middle) \mathbf{H}_2 -eigenvector for the eigenvalue 0. Both eigenvectors are examples for the construction method described in step 2. (Right) \mathbf{H}_2 -eigenvector for the eigenvalue 0. This eigenvector is an example for the construction method described in step 3. The number assigned to a vertex is the value of the eigenvector at this vertex.

5. TWO EXAMPLES

In this section, we demonstrate the applicability of theorem 4.9 on two models of Diamond-type graphs. A transversal decomposition of each of these models induces a 1D chain D_N . We equip D_N with a Jacobi matrix \mathbf{J} of one of the simplest cases of spin chains with perfect state transfer discussed in [CDEL04]. To this end, we set

$$(5.1) \quad J_n = \frac{\sqrt{n(N+1-n)}}{2}, \quad B_n = 0, \quad n = 0, 1, \dots, N, \quad B_{N+1} = 0,$$

for the entries in (3.2). The underlying Jacobi matrix is mirror symmetric and it corresponds to the symmetric Krawtchouk polynomials [Sze75]. Following Proposition 2.14, we lift this Jacobi matrix to Hamiltonians on these models of Diamond-type graphs. Note that the magnetic field on the 1D chain nodes is assumed to vanish $B_0 = \dots = B_{N+1} = 0$, resulting in a Hamiltonian whose diagonal elements are all equal to zero.

Moreover, Theorem 2.12 implies that such Hamiltonians achieve a perfect quantum state transfer. We investigate the Hamiltonians explicitly provide a complete description of their spectra.

$$(5.2) \quad \mathbf{J}_2 = \begin{bmatrix} 0 & 1 & 0 & 0 & 0 \\ 1 & 0 & \frac{\sqrt{6}}{2} & 0 & 0 \\ 0 & \frac{\sqrt{6}}{2} & 0 & \frac{\sqrt{6}}{2} & 0 \\ 0 & 0 & \frac{\sqrt{6}}{2} & 0 & 1 \\ 0 & 0 & 0 & 1 & 0 \end{bmatrix}$$

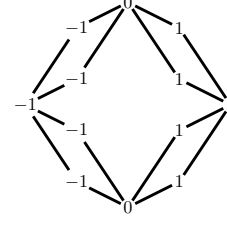


FIGURE 6. An example of a radial eigenvector of \mathbf{H}_2 . It corresponds to the eigenvalue 1. The number assigned to a vertex is the value of the eigenvector at this vertex.

5.1. Hambly-Kumagai diamond graphs. The first model is an example of a two-point self-similar graph in the sense of [MT95]. It is a particular sequence of Diamond-type graphs, that was investigated in [HK10]. We will refer to this model as *Hambly-Kumagai diamond graphs*. The following definition gives a formal description of the Hambly-Kumagai diamond graphs.

Definition 5.1. We refer to a sequence of graphs $\{HK_\ell\}_{\ell \geq 0}$ as *Hambly-Kumagai Diamond graphs*, when it is constructed as follows.

- HK_0 is initialized as the one edge graph connecting a node x_L with another node x_R .
- At level ℓ we construct HK_ℓ by replacing each edge from the previous level $HK_{\ell-1}$ by two new branches, whereas each new branch is then segmented into two edges that are arranged in series.

The first three levels of the Hambly-Kumagai diamond graphs are displayed in [DDMT19, Figure 2, page 5]. Let $V(HK_\ell)$ be the vertices set of HK_ℓ . It is easily seen that the transversal decomposition $V(HK_\ell) = \Pi_A^{-1}(0) \cup \Pi_A^{-1}(1) \dots \cup \Pi_A^{-1}(N)$ with respect to $A = \{x_L\}$ induces a 1D chain D_N , such that $N = 2^\ell$. The Jacobi matrix associated with D_N , $N = 2^\ell$ is denoted by \mathbf{J}_ℓ . For example \mathbf{J}_2 is given in equation (5.2). We lift \mathbf{J}_ℓ to a Hamiltonian \mathbf{H}_ℓ on HK_ℓ . The Hamiltonian \mathbf{H}_2 on the Hambly-Kumagai diamond graph of level 2 is given in equation (5.3).

$$(5.3) \quad \mathbf{H}_2 = \begin{bmatrix} 0 & 0 & 0 & 0 & \frac{1}{4} & \frac{1}{4} & \frac{1}{4} & \frac{1}{4} & 0 & 0 & 0 & 0 \\ 0 & 0 & 0 & 0 & 0 & 0 & 0 & 0 & \frac{1}{4} & \frac{1}{4} & \frac{1}{4} & \frac{1}{4} \\ 0 & 0 & 0 & 0 & \frac{\sqrt{6}}{4} & \frac{\sqrt{6}}{4} & 0 & 0 & \frac{\sqrt{6}}{4} & \frac{\sqrt{6}}{4} & 0 & 0 \\ 0 & 0 & 0 & 0 & 0 & 0 & \frac{\sqrt{6}}{4} & \frac{\sqrt{6}}{4} & 0 & 0 & \frac{\sqrt{6}}{4} & \frac{\sqrt{6}}{4} \\ 1 & 0 & \frac{\sqrt{6}}{2} & 0 & 0 & 0 & 0 & 0 & 0 & 0 & 0 & 0 \\ 1 & 0 & \frac{\sqrt{6}}{2} & 0 & 0 & 0 & 0 & 0 & 0 & 0 & 0 & 0 \\ 1 & 0 & 0 & \frac{\sqrt{6}}{2} & 0 & 0 & 0 & 0 & 0 & 0 & 0 & 0 \\ 1 & 0 & 0 & \frac{\sqrt{6}}{2} & 0 & 0 & 0 & 0 & 0 & 0 & 0 & 0 \\ 0 & 1 & \frac{\sqrt{6}}{2} & 0 & 0 & 0 & 0 & 0 & 0 & 0 & 0 & 0 \\ 0 & 1 & \frac{\sqrt{6}}{2} & 0 & 0 & 0 & 0 & 0 & 0 & 0 & 0 & 0 \\ 0 & 1 & 0 & \frac{\sqrt{6}}{2} & 0 & 0 & 0 & 0 & 0 & 0 & 0 & 0 \\ 0 & 1 & 0 & \frac{\sqrt{6}}{2} & 0 & 0 & 0 & 0 & 0 & 0 & 0 & 0 \end{bmatrix}$$

5.1.1. Spectrum of the Hamiltonian \mathbf{H}_2 . In this section we demonstrate how to apply Theorem 4.9 and determine the spectrum of \mathbf{H}_2 . To this end, we construct the level-2 Hambly-Kumagai diamond graph HK_2 using a sequence of discretized projective limit spaces $\{G_0, G_1, G_2\}$ (see Definition 4.4) such that $HK_2 = G_2$. We proceed with the following steps:

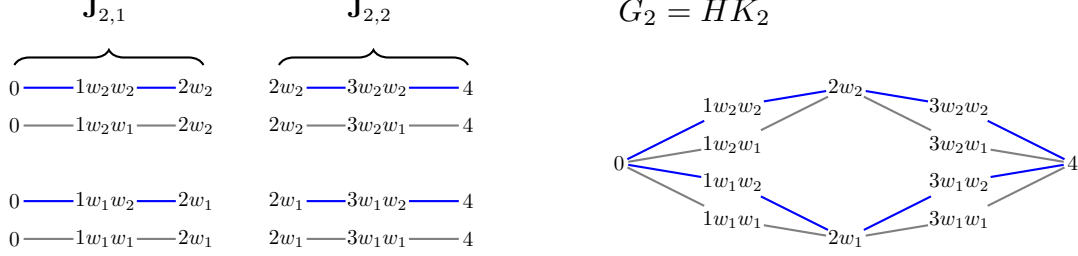


FIGURE 7. (Right) We set G_1 to be the graph shown in Figure 3. G_2 is constructed as described in Figure 4 (Right), namely by taking the two copies $G_1 \times \{w_1\}$, $G_1 \times \{w_2\}$ and choosing the subgraph B_2 such that $V(B_2) = \{0, 2w_1, 2w_2, 4\}$ and $E(B_2) = \emptyset$. Note that G_2 is the level-2 Hambly-Kumagai Diamond graph and denoted by HK_2 . (Left) It is easy to see that $G_1 \setminus B_2$ is a collection of four 1D chains. The two copies of each 1D chain in $G_1 \setminus B_2$ are displayed in Figure. Each 1D chain in $G_1 \setminus B_2$ is associated with a Jacobi matrix. Due to the mirror symmetry assumption, there are only two different Jacobi matrices. We denote them by $\mathbf{J}_{2,1}$ and $\mathbf{J}_{2,2}$.

- (Step 1) G_0 is initialized to be the induced auxiliary 1D chain D_4 equipped \mathbf{J}_2 given in (5.2). Let $\lambda \in \sigma(\mathbf{J}_2)$ with v_λ as the corresponding eigenvector. Then $P_2^* v_\lambda = \phi_1^* \phi_2^* v_\lambda$ gives a corresponding radial \mathbf{H}_2 -eigenvector on HK_2 (by Lemma 3.1 or 4.8). Figure 6 displays a radial eigenvector of \mathbf{H}_2 corresponding to the eigenvalue 1. It describes the oscillations of the transversal layers. This step shows $\sigma(\mathbf{J}_2) \subset \sigma(\mathbf{H}_2)$ and generates five radial eigenvectors. Note that $\sigma(\mathbf{J}_2) = \{-2, -1, 0, 1, 2\}$, see Table 1 (Left).
- (Step 2) To construct the graph G_1 , we proceed as described in Figure 3 (Left). This is precisely the situation described in Lemma 3.6 (Lifting & Gluing Lemma), where G_1 plays the role of G_D with two branches. Hence, we can lift an eigenvector from G_0 to G_1 as follows. Recall, when Dirichlet boundary conditions are imposed, we write \mathbf{J}_2^D for the Jacobi matrix. Let $\lambda \in \sigma(\mathbf{J}_2^D)$ with v_λ^D as the corresponding \mathbf{J}_2^D -eigenvector. Then, the vector

$$v_\lambda = \begin{cases} v_\lambda^D & \text{on the } w_1\text{-branch} \\ -v_\lambda^D & \text{on the } w_2\text{-branch} \end{cases}$$

defines an eigenvector on G_1 . Lifting v_λ to HK_2 via $\phi_2^* v_\lambda$ gives an eigenvector of \mathbf{H}_2 (see Lemma 4.8). Figures 5 (left) & (middle) display eigenvectors of \mathbf{H}_2 constructed as described in step 2. This step shows $\sigma(\mathbf{J}_2^D) \subset \sigma(\mathbf{H}_2)$ and generates three additional eigenvectors. Note that $\sigma(\mathbf{J}_2^D) = \{-\sqrt{3}, 0, \sqrt{3}\}$, see Table 1 (Middle).

- (Step 3) To construct the level-2 Hambly-Kumagai graph $G_2 = HK_2$, we proceed as described in Definition 4.4 and Figure 7. For the vertical multiplier space, we set $W = \{w_1, w_2\}$. We choose the subgraph B_2 to be edgeless with the vertices set $V(B_2) = \{0, 2w_1, 2w_2, 4\}$. In this case, $G_1 \setminus B_2$ is a collection of four 1D chains. The two copies of each 1D chain in $G_1 \setminus B_2$ are displayed in Figure 7 (Left). Gluing the copies at the common boundary vertices gives $G_2 = HK_2$, see Figure 7 (Right). Each 1D chain in $G_1 \setminus B_2$ is associated with a Jacobi matrix. Due to the mirror symmetry assumption, it is sufficient to consider one of the four Jacobi matrices. We denote this Jacobi matrix by $\mathbf{J}_{2,1}$, see Figure 7 (Left). It is easy to check that $\mathbf{J}_{2,1}$ is given by

$$\mathbf{J}_{2,1} = \begin{bmatrix} 0 & 1 & 0 \\ 1 & 0 & \frac{\sqrt{6}}{2} \\ 0 & \frac{\sqrt{6}}{2} & 1 \end{bmatrix}$$

Gluing two copies of a 1D chain in $G_1 \setminus B_2$ generates a similar situation to Lemma 3.6 (Lifting & Gluing Lemma). Hence, we can lift an eigenvector to G_2 as follows. Let $\lambda \in \sigma(\mathbf{J}_{2,1}^D)$ with v_λ^D as the

corresponding \mathbf{J}_2^D -eigenvector. We define

$$v_\lambda = \begin{cases} v_\lambda^D & \text{on the } w_1\text{-branch of a } 1D \text{ chain in } G_1 \setminus B_2 \\ -v_\lambda^D & \text{on the } w_2\text{-branch of the same } 1D \text{ chain in } G_1 \setminus B_2 \\ 0 & \text{elsewhere} \end{cases}$$

It is easy to see that v_λ defines an eigenvector on \mathbf{H}_2 . This step shows $\sigma(\mathbf{J}_{2,1}^D) \subset \sigma(\mathbf{H}_2)$ and generates four additional eigenvectors, one eigenvector for each $1D$ chain in $G_1 \setminus B_2$. Note that $\sigma(\mathbf{J}_{2,1}^D) = \{0\}$. The constructed twelve eigenvectors are orthogonal and therefore $\sigma(\mathbf{H}_2) = \sigma(\mathbf{J}_2) \cup \sigma(\mathbf{J}_2^D) \cup \sigma(\mathbf{J}_{2,1}^D)$.

Eigenvalue Multiplicity						Eigenvalue Multiplicity		
1	-2	1				1	-2	1
2	-1	1				2	$-\sqrt{3}$	1
3	0	1				3	-1	1
4	1	1				4	0	6
5	2	1				5	1	1
						6	$\sqrt{3}$	1
						7	2	1

TABLE 1. Hambly-Kumagai diamond graph of level 2: Eigenvalues table of \mathbf{J}_2 (Left), \mathbf{J}_2^D (Middle) and of \mathbf{H}_2 (Right).

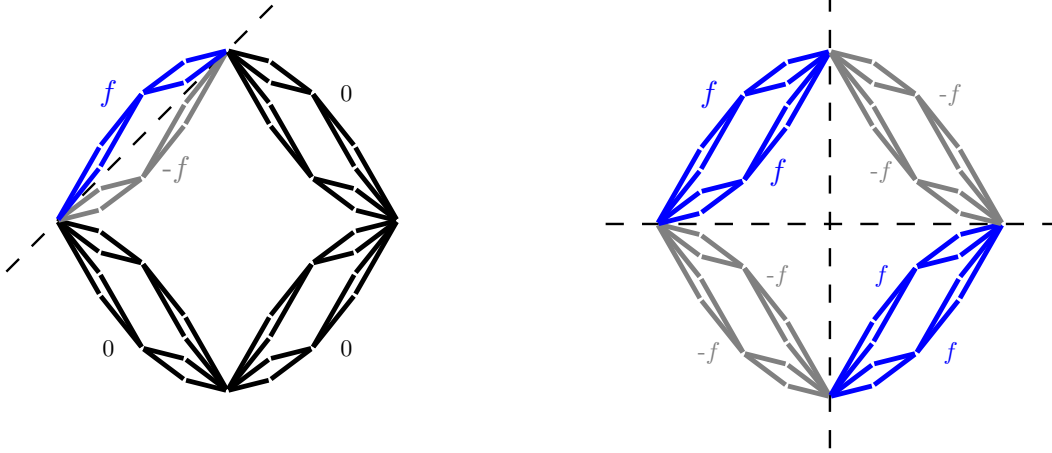


FIGURE 8. Eigenvalues of multiplicity five: (Left) With an argument similar to Lemma 3.6 (Lifting-&-Gluing), we can lift a Dirichlet eigenvector f of a particular Jacobi submatrix to the subgraph colored blue. Moreover, we lift the same eigenvector but with the opposite sign to the subgraph colored gray. The constructed vector is then an eigenvector of \mathbf{H}_ℓ with the same eigenvalue. In this way, we can construct a total of four eigenvectors to the same eigenvalue. (Right) Lifting the same eigenvector as described in the right-hand side Figure will result in the fifth eigenvector of \mathbf{H}_ℓ with the same eigenvalue.

Proposition 5.2. *Let $\ell \geq 3$. There exists $\lambda \in \sigma(\mathbf{H}_\ell)$, such that the multiplicity of λ is 5.*

Proof. Using an argument similar to Lemma 3.6 (Lifting-&-Gluing) and Figure 8. □

We will refer to eigenvectors of \mathbf{H}_ℓ that are supported on a proper subset of $V(HK_\ell)$ as localized eigenvectors.

Proposition 5.3. *The total number of localized eigenvectors of \mathbf{H}_ℓ is $\frac{2 \cdot 4^\ell + 4}{3} - 2^\ell - 2^{\ell-1}$, $\ell \geq 3$.*

Proof. The number of vertices of HK_ℓ at level $\ell \in \mathbb{N}$ is $|V(HK_\ell)| = \frac{2 \cdot 4^\ell + 4}{3}$. The algorithm or ideas above illustrates how to construct the eigenvectors. In particular, it shows that the only non-localized eigenvectors are the $2^\ell + 1$ radial eigenvectors and the $2^{\ell-1} - 1$ “fifth” eigenvectors in Figure 8 (Right). \square

We can proceed similarly for higher levels and compute the spectrum by considering a collection of Jacobi matrices. A convenient representation of the higher levels spectrum is to plot the *integrated density of states* of \mathbf{H}_ℓ , that is defined as

$$N_\ell(x) := \frac{\#\{\lambda \leq x \mid \lambda \text{ is an eigenvalue of } \mathbf{H}_\ell\}}{|V(HK_\ell)|},$$

where $\#$ counts the number of eigenvalues of \mathbf{H}_ℓ less or equal than x . Figure 9 shows the integrated density of states of \mathbf{H}_ℓ for both level 6 (Left) and level 7 (Right).

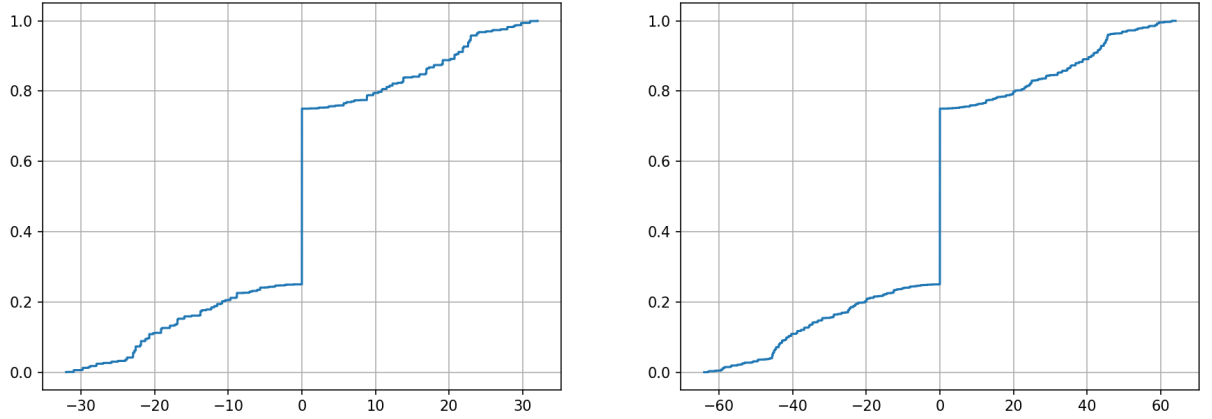


FIGURE 9. Integrated density of states of \mathbf{H}_ℓ : Hambly-Kumagai diamond graph of level 6 (Left) and level 7 (Right).

5.2. Lang-Plaut Diamond graphs. The second model is also an example of a two-point self-similar graph in the sense of [MT95]. It is another prominent example of Diamond-type graphs, that was investigated in [LP01]. We will refer to this model as *Lang-Plaut diamond graphs*. The following definition gives a formal description of the Lang-Plaut diamond graphs.

Definition 5.4. We refer to a sequence of graphs $\{LP_\ell\}_{\ell \geq 0}$ as *Lang-Plaut diamond graphs*, when it is constructed as follows.

- LP_0 is initialized as the one edge graph connecting a node x_L with another node x_R .
- At level ℓ , we construct LP_ℓ by segmenting each edge from the previous level $LP_{\ell-1}$ into three new edges. The inner edge of the three new edges is then replaced by two new branches, whereas each new branch is then segmented into two edges.

The first four levels of the Lang-Plaut diamond graphs are displayed in [DDMT19, Figure 4, page 10]. Let $V(LP_\ell)$ be the vertices set of LP_ℓ . In the same manner as the Hambly-Kumagai diamond graphs, it is easily seen that the transversal decomposition $V(LP_\ell) = \Pi_A^{-1}(0) \cup \Pi_A^{-1}(1) \dots \cup \Pi_A^{-1}(N)$ with respect to $A = \{x_L\}$ induces a 1D chain D_N , such that $N = 4^\ell$. The Jacobi matrix associated with D_N , $N = 4^\ell$ is denoted by \mathbf{J}_ℓ . We lift \mathbf{J}_ℓ to a Hamiltonian \mathbf{H}_ℓ on LP_ℓ .

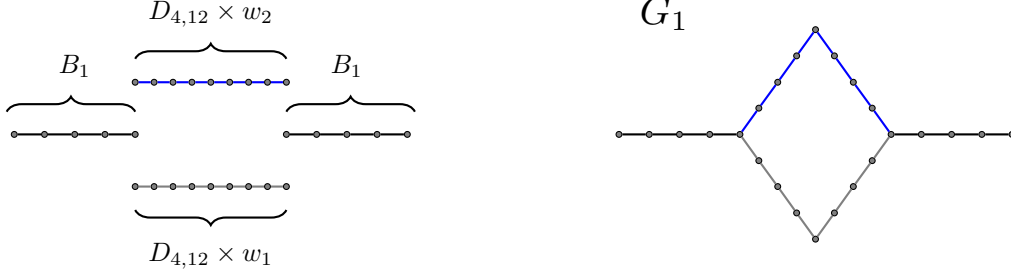


FIGURE 10. (Left) To construct G_1 we take two copies of the 1D chain $G_0 = D_{16}$ (Recall the vertices set is $V(D_{16}) = \{0, \dots, 16\}$) and choose the subgraph B_1 such that $G_0 \setminus B_1$ contains only the 1D chain with the set of vertices $V(D_{4,12}) = \{4, 5, \dots, 12\}$. We will refer to this 1D chain as $D_{4,12}$. For the vertical multiplier space we set $W = \{w_1, w_2\}$. (Right) G_1 is given by gluing the two copies $D_{4,12} \times \{w_1\}$ and $D_{4,12} \times \{w_2\}$ together with B_1 at their boundary points.

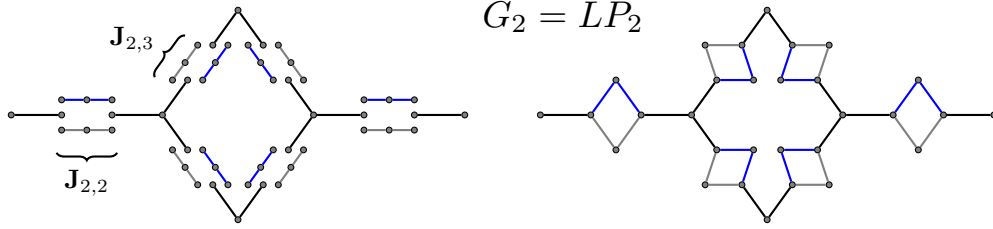


FIGURE 11. (Left) The Jacobi matrices $\mathbf{J}_{2,3}$ and $\mathbf{J}_{2,2}$ are relevant for the computation of $\sigma(\mathbf{H}_2)$. (Right) Lang-Plaut diamond graphs of level-2, $G_2 = HK_2$.

5.2.1. *Spectrum of the Hamiltonian \mathbf{H}_2 .* We proceed as in the first model and demonstrate how to apply Theorem 4.9 while determining the spectrum of \mathbf{H}_2 . Similarly, we construct the level-2 Lang-Plaut diamond graph LP_2 using a sequence of discretized projective limit spaces $\{G_0, G_1, G_2\}$ (see Definition 4.4) such that $LP_2 = G_2$. We proceed with the following steps:

- (Step 1) G_0 is initialized to be the induced auxiliary 1D chain D_{16} equipped \mathbf{J}_2 , with entries given in (5.1). Similar to the first model we can show $\sigma(\mathbf{J}_2) \subset \sigma(\mathbf{H}_2)$ and generate 17 radial eigenvectors. Note that $\sigma(\mathbf{J}_2) = \{-8, -7, \dots, 7, 8\}$, see Table 2 (Left).
- (step 2) To construct the graph G_1 , we proceed as described in Figure 10. Again, with a similar argument to the Lifting & Gluing Lemma, we lift an eigenvector from the 1D chain $D_{4,12}$ to G_2 . We denote the Jacobi matrix associated with $D_{4,12}$ by

$$\mathbf{J}_{2,1} = \begin{bmatrix} 0 & \sqrt{15} & 0 & 0 & 0 & 0 & 0 & 0 & 0 \\ \sqrt{15} & 0 & \frac{\sqrt{66}}{2} & 0 & 0 & 0 & 0 & 0 & 0 \\ 0 & \frac{\sqrt{66}}{2} & 0 & \frac{\sqrt{70}}{2} & 0 & 0 & 0 & 0 & 0 \\ 0 & 0 & \frac{\sqrt{70}}{2} & 0 & 3\sqrt{2} & 0 & 0 & 0 & 0 \\ 0 & 0 & 0 & 3\sqrt{2} & 0 & 3\sqrt{2} & 0 & 0 & 0 \\ 0 & 0 & 0 & 0 & 3\sqrt{2} & 0 & \frac{\sqrt{70}}{2} & 0 & 0 \\ 0 & 0 & 0 & 0 & 0 & \frac{\sqrt{70}}{2} & 0 & \frac{\sqrt{66}}{2} & 0 \\ 0 & 0 & 0 & 0 & 0 & 0 & \frac{\sqrt{66}}{2} & 0 & \sqrt{15} \\ 0 & 0 & 0 & 0 & 0 & 0 & 0 & \sqrt{15} & 0 \end{bmatrix}$$

Similar to the first model we can show $\sigma(\mathbf{J}_{2,1}^D) \subset \sigma(\mathbf{H}_2)$ and generate 7 additional eigenvectors. The eigenvalues \mathbf{J}_2^D are listed in Table 2 (Middle).

- (step 3) To construct finally the level-2 Lang-Plaut diamond graphs $G_2 = HK_2$, we proceed similarly to the first model. The relevant Jacobi matrices $\mathbf{J}_{2,2}$ and $\mathbf{J}_{2,3}$ are indicated in Figure 11 (Left). Again,

due to the mirror symmetry, it is sufficient to consider two out of six matrices. We can show $\sigma(\mathbf{J}_{2,2}), \sigma(\mathbf{J}_{2,3}) \subset \sigma(\mathbf{H}_2)$ and generate 6 additional eigenvectors. Note that $\sigma(\mathbf{J}_{2,2}^D) = \sigma(\mathbf{J}_{2,3}^D) = \{0\}$. The generated 30 eigenvectors are orthogonal. Hence $\sigma(\mathbf{H}_2) = \sigma(\mathbf{J}_2) \cup \sigma(\mathbf{J}_{2,1}^D) \cup \sigma(\mathbf{J}_{2,2}^D) \cup \sigma(\mathbf{J}_{2,3}^D)$. Figure 12 shows the integrated density of states of \mathbf{H}_ℓ for both level 4 (Left) and level 5 (Right).

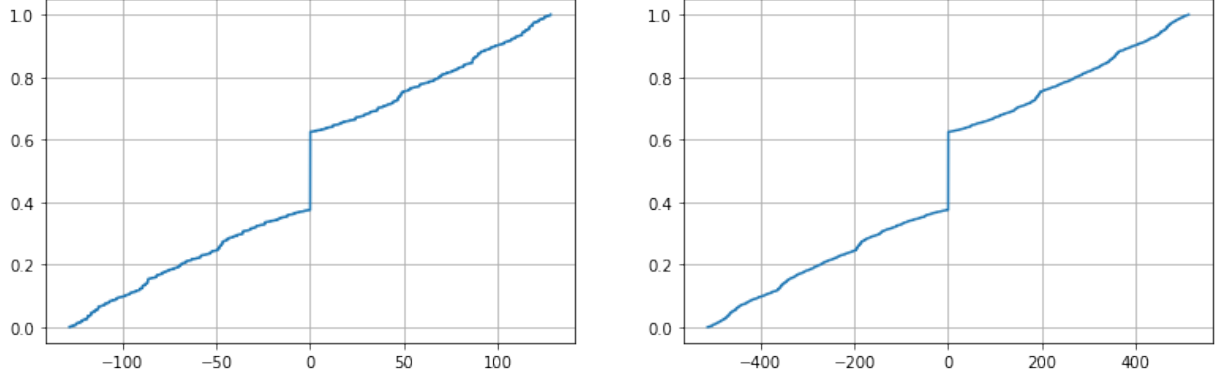


FIGURE 12. Integrated density of states of \mathbf{H}_ℓ : Lang-Plaut diamond graph of level 4 (left) and level 5 (right).

Eigenvalue Multiplicity			Eigenvalue Multiplicity		
1	-8.0	1	1	-7.7536903	1
2	-7.0	1	2	-5.8309519	1
3	-6.0	1	3	-3.1432923	1
4	-5.0	1	4	0.0	1
5	-4.0	1	5	3.1432923	1
6	-3.0	1	6	5.8309519	1
7	-2.0	1	7	7.7536903	1
8	-1.0	1			
9	0.0	1			
10	1.0	1			
11	2.0	1			
12	3.0	1			
13	4.0	1			
14	5.0	1			
15	6.0	1			
16	7.0	1			
17	8.0	1			

Eigenvalue Multiplicity		
1	-8.0	1
2	-7.753690	1
3	-7.0	1
4	-6.0	1
5	-5.830951	1
6	-5.0	1
7	-4.0	1
8	-3.143292	1
9	-3.0	1
10	-2.0	1
11	-1.0	1
12	0.0	8
13	1.0	1
14	2.0	1
15	3.0	1
16	3.143292	1
17	4.0	1
18	5.0	1
19	5.830951	1
20	6.0	1
21	7.0	1
22	7.753690	1
23	8.0	1

TABLE 2. Lang-Plaut Diamond graphs of level 2: Eigenvalues table of \mathbf{J}_2 (Left), $\mathbf{J}_{2,1}^D$ (Middle) and of \mathbf{H}_2 (Right).

6. FURTHER GENERAL GEOMETRIC CONSTRUCTIONS: TWO-POINT SELF SIMILAR GRAPHS

In [MT95] a broad class of infinite self-similar graphs called *two-point self-similar fractal graphs* was introduced and the spectra of the combinatorial- and probabilistic-Laplacians on such graphs were described. The two-point self-similar fractal graphs are related to the nested fractals with two essential fixed points [LL90]. A generalization to self-similar graphs based on a finite symmetric M -point model (instead of two points) is constructed in [MT03].

Following [MT95], we set $M = (V_M, E_M)$ and $G_0 = (V_0, E_0)$ to be finite connected graphs, where M is an ordered graph. We fix some $e_0 \in E_M$, which is not a loop, and vertices $\alpha, \beta \in V_M$ and $\alpha_0, \beta_0 \in V_0$, $\alpha \neq \beta$, $\alpha_0 \neq \beta_0$.

Definition 6.1 ([MT95], page 393). A graph G is called *two point self-similar graph* with model graph M and initial graph G_0 if the following holds:

- (1) There are finite subgraphs $\{G_n\}_{n \geq 0}$, $G_n = (V_n, E_n)$ such that $G_n \subset G_{n+1}$, $n \geq 0$, and $G = \bigcup_{n \geq 0} G_n$.
- (2) For any $n \geq 0$ and $e \in E_M$ there is a graph homomorphism $\Psi_n^e : G_n \rightarrow G_{n+1}$ such that $G_{n+1} = \bigcup_{e \in E_M} \Psi_n^e(G_n)$ and $\Psi_n^{e_0}$ is the inclusion of G_n to G_{n+1} .
- (3) For all $n \geq 0$ there are two vertices $\alpha_n, \beta_n \in V_n$ such that Ψ_n^e restricted to $G_n \setminus \{\alpha_n, \beta_n\}$ is a one-to-one mapping for every $e \in E_M$. Moreover $\Psi_n^{e_1}(V_n \setminus \{\alpha_n, \beta_n\}) \cap \Psi_n^{e_2}(V_n \setminus \{\alpha_n, \beta_n\}) = \emptyset$ if $e_1 \neq e_2$.
- (4) For $n \geq 1$, there is an injection $\kappa_n : V_M \rightarrow V_n$ such that $\alpha_n = \kappa_n(\alpha)$, $\beta_n = \kappa_n(\beta)$ and for every edge $e = (a, b) \in E_M$, $\Psi_{n-1}^e(\alpha_{n-1}) = \kappa_n(a)$ and $\Psi_{n-1}^e(\beta_{n-1}) = \kappa_n(b)$.

We say that the vertices α_n, β_n are the boundary vertices of G_n , i.e. $\partial G_n = \{\alpha_n, \beta_n\}$ and $\text{int}(G_n) = V_n \setminus \{\alpha_n, \beta_n\}$ are the interior vertices of G_n .

Proposition 6.2. Suppose that the graphs M and G_0 satisfy the assumptions 2.10, where the transversal decomposition of M and G_0 are with respect α (or β) and α_0 (or β_0), respectively. Moreover, we assume $\deg_0(x) = 0$ for all $x \in V_M$. Then the assumptions 2.10 hold for each G_i , $i \geq 0$. And the transversal decomposition of G_i is with respect α_i (or β_i).

Proof. $G_{\ell+1}$ is obtained by replacing every edge in M by a copy of G_ℓ . Under the assumptions, the transversal decomposition of M with respect α (or β) is modified by adding the transversal layers of G_ℓ resulting in a transversal decomposition of $G_{\ell+1}$ with respect $\alpha_{\ell+1}$ (or $\beta_{\ell+1}$). \square

ACKNOWLEDGMENTS

This research was supported in part by the University of Connecticut Research Excellence Program, by DOE grant DE-SC0010339 and by NSF DMS grant 1613025.

REFERENCES

- [ABD⁺12] Eric Akkermans, Olivier Benichou, Gerald V Dunne, Alexander Teplyaev, and Raphael Voituriez. Spatial log-periodic oscillations of first-passage observables in fractals. *Physical Review E*, 86(6):061125, 2012. 2
- [ACD⁺19] Eric Akkermans, Joe P Chen, Gerald Dunne, Luke G Rogers, and Alexander Teplyaev. Fractal AC circuits and propagating waves on fractals. *to appear in the 6th Cornell Fractals Conference Proceedings, arXiv:1507.05682*, 2019. 2
- [ACNO⁺10] Ricardo J. Angeles-Canul, Rachael M. Norton, Michael C. Opperman, Christopher C. Paribello, Matthew C. Russell, and Christino Tamon. Perfect state transfer, integral circulants, and join of graphs. *Quantum Inf. Comput.*, 10(3-4):325–342, 2010. 2
- [ADT09] Eric Akkermans, Gerald V Dunne, and Alexander Teplyaev. Physical consequences of complex dimensions of fractals. *EPL (Europhysics Letters)*, 88(4):40007, 2009. 2
- [ADT10] Eric Akkermans, Gerald V Dunne, and Alexander Teplyaev. Thermodynamics of photons on fractals. *Physical review letters*, 105(23):230407, 2010. 2
- [Akk13] Eric Akkermans. Statistical mechanics and quantum fields on fractals. In *Fractal geometry and dynamical systems in pure and applied mathematics. II. Fractals in applied mathematics*, volume 601 of *Contemp. Math.*, pages 1–21. Amer. Math. Soc., Providence, RI, 2013. 2
- [AR18] Patricia Alonso Ruiz. Explicit formulas for heat kernels on diamond fractals. *Comm. Math. Phys.*, 364(3):1305–1326, 2018. 2
- [AR19] Patricia Alonso Ruiz. Heat kernel analysis on diamond fractals. *Preprint*, 2019. 2
- [ARHTT18] Patricia Alonso-Ruiz, Michael Hinz, Alexander Teplyaev, and Rodrigo Treviño. Canonical diffusions on the pattern spaces of aperiodic delone sets. *Preprint arXiv:1801.08956*, 2018. 2
- [ARKT16] Patricia Alonso-Ruiz, Daniel J. Kelleher, and Alexander Teplyaev. Energy and Laplacian on Hanoi-type fractal quantum graphs. *J. Phys. A*, 49(16):165206, 36, 2016. 2

- [BB05a] Daniel Burgarth and Sougato Bose. Conclusive and arbitrarily perfect quantum-state transfer using parallel spin-chain channels. *Physical Review A*, 71(5):052315, 2005. [2](#)
- [BB05b] Daniel Burgarth and Sougato Bose. Perfect quantum state transfer with randomly coupled quantum chains. *New journal of physics*, 7(1):135, 2005. [2](#)
- [BCD⁺08a] N. Bajorin, T. Chen, A. Dagan, C. Emmons, M. Hussein, M. Khalil, P. Mody, B. Steinhurst, and A. Teplyaev. Vibration modes of $3n$ -gaskets and other fractals. *J. Phys. A*, 41(1):015101, 21, 2008. [2](#)
- [BCD⁺08b] N. Bajorin, T. Chen, A. Dagan, C. Emmons, M. Hussein, M. Khalil, P. Mody, B. Steinhurst, and A. Teplyaev. Vibration spectra of finitely ramified, symmetric fractals. *Fractals*, 16(3):243–258, 2008. [2](#)
- [BCH⁺17] Antoni Brzoska, Aubrey Coffey, Madeline Hansalik, Stephen Loew, and Luke G Rogers. Spectra of magnetic operators on the diamond lattice fractal. *Preprint arXiv:1704.01609*, 2017. [2](#)
- [BE04] Martin T. Barlow and Steven N. Evans. Markov processes on vermiculated spaces. In *Random walks and geometry*, pages 337–348. Walter de Gruyter, Berlin, 2004. [2](#)
- [BFF⁺12] Rachel Bachman, Eric Fredette, Jessica Fuller, Michael Landry, Michael Opperman, Christino Tamon, and Andrew Tollefson. Perfect state transfer on quotient graphs. *Quantum Inf. Comput.*, 12(3-4):293–313, 2012. [2](#)
- [BGS08] Anna Bernasconi, Chris Godsil, and Simone Severini. Quantum networks on cubelike graphs. *Phys. Rev. A* (3), 78(5):052320, 5, 2008. [2](#)
- [BO79] A N Berker and S Ostlund. Renormalisation-group calculations of finite systems: order parameter and specific heat for epitaxial ordering. *Journal of Physics C: Solid State Physics*, 12(22):4961–4975, nov 1979. [2](#)
- [Bos03] Sougato Bose. Quantum communication through an unmodulated spin chain. *Physical Review Letters*, 91(20):207901, 2003. [1](#)
- [Bos07] Sougato Bose. Quantum Communication through Spin Chain Dynamics: an Introductory Overview. *Contemporary Physics*, 48:13 – 30, Feb 2007. [1](#), [2](#)
- [CDEL04] Matthias Christandl, Nilanjana Datta, Artur Ekert, and Andrew J Landahl. Perfect state transfer in quantum spin networks. *Physical Review Letters*, 92(18):187902, 2004. [2](#), [11](#)
- [CK13a] Jeff Cheeger and Bruce Kleiner. Inverse limit spaces satisfying a poincaré inequality. *Analysis and Geometry in Metric Spaces*, 3, 2013. [2](#)
- [CK13b] Jeff Cheeger and Bruce Kleiner. Realization of metric spaces as inverse limits, and bilipschitz embedding in \mathbb{R}^n . *Geometric and Functional Analysis*, 23(1):96–133, Feb 2013. [2](#)
- [Col85] P. Collet. *Systems with Random Couplings on Diamond Lattices*, pages 105–126. Birkhäuser Boston, Boston, MA, 1985. [2](#)
- [CVZ17] Matthias Christandl, Luc Vinet, and Alexei Zhedanov. Analytic next-to-nearest-neighbor $x \times x$ models with perfect state transfer and fractional revival. *Physical Review A*, 96(3):032335, 2017. [1](#)
- [DdI83] B. Derrida, L. de Seze, and C. Itzykson. Fractal structure of zeros in hierarchical models. *Journal of Statistical Physics*, 33(3):559–569, Dec 1983. [2](#)
- [DDMT19] Maxim Derevyagin, Gerald V. Dunne, Gamal Mograby, and Alexander Teplyaev. Perfect quantum state transfer on diamond fractal graphs. *arXiv e-prints*, page arXiv:1909.08668, Sep 2019. [2](#), [3](#), [4](#), [6](#), [12](#), [15](#)
- [Dun12] Gerald V. Dunne. Heat kernels and zeta functions on fractals. *J. Phys. A*, 45(37):374016, 22, 2012. [2](#)
- [GKH⁺01] Gerhard R. Guthöhrlein, Matthias Keller, Kazuhiro Hayasaka, Wolfgang Lange, and Herbert Walther. A single ion as a nanoscopic probe of an optical field. *Nature*, 414:49–51, 2001. [1](#)
- [God12a] Chris Godsil. State transfer on graphs. *Discrete Math.*, 312(1):129–147, 2012. [2](#)
- [God12b] Chris Godsil. When can perfect state transfer occur? *Electron. J. Linear Algebra*, 23:877–890, 2012. [2](#)
- [HK10] B. M. Hambly and T. Kumagai. Diffusion on the scaling limit of the critical percolation cluster in the diamond hierarchical lattice. *Comm. Math. Phys.*, 295(1):29–69, 2010. [2](#), [12](#)
- [HM19] Michael Hinz and Melissa Meinert. On the viscous Burgers equation on metric graphs and fractals. *Journal of Fractal Geometry*, to appear. *arXiv:1712.05472*, 2019. [2](#)
- [HO07] Akihito Hora and Nobuaki Obata. *Quantum probability and spectral analysis of graphs*. Theoretical and Mathematical Physics. Springer, Berlin, 2007. With a foreword by Luigi Accardi. [3](#), [7](#)
- [Kay74] A Kay. A review of perfect state transfer and its applications as a constructive tool. *Int. J. Quantum Inform.*, 641(8), 2010. Preprint quant-ph/0903.4274. [1](#), [2](#)
- [KLY17a] Mark Kempton, Gabor Lippner, and Shing-Tung Yau. Perfect state transfer on graphs with a potential. *Quantum Inf. Comput.*, 17(3-4):303–327, 2017. [1](#), [2](#)
- [KLY17b] Mark Kempton, Gabor Lippner, and Shing-Tung Yau. Pretty good quantum state transfer in symmetric spin networks via magnetic field. *Quantum Inf. Process.*, 16(9):Art. 210, 23, 2017. [2](#)
- [KMP⁺19] Steve Kirkland, Darian McLaren, Rajesh Pereira, Sarah Plosker, and Xiaohong Zhang. Perfect quantum state transfer in weighted paths with potentials (loops) using orthogonal polynomials. *Linear Multilinear Algebra*, 67(5):1043–1061, 2019. [2](#)
- [KS05] Peter Karbach and Joachim Stolze. Spin chains as perfect quantum state mirrors. *Physical Review A*, 72(3):030301, 2005. [2](#)
- [LDM⁺03] D Leibfried, B DeMarco, V Meyer, D Lucas, Murray Barrett, J Britton, Wayne Itano, Brana Jelenkovic, Chris Langer, T. Rosenband, and D Wineland. Experimental demonstration of a robust, high-fidelity geometric two ion-qubit phase gate. *Nature*, 422:412–5, 04 2003. [1](#)
- [LL90] T. Lindström and T. Lindström. *Brownian Motion on Nested Fractals*. American Mathematical Society: Memoirs of the American Mathematical Society. American Mathematical Society, 1990. [18](#)
- [LP01] Urs Lang and Conrad Plaut. Bilipschitz embeddings of metric spaces into space forms. *Geom. Dedicata*, 87(1-3):285–307, 2001. [15](#)

- [LTS83] J. M. Langlois, A. M. Tremblay, and B. W. Southern. Chaotic scaling trajectories and hierarchical lattice models of disordered binary harmonic chains. *Phys. Rev. B*, 28:218–231, Jul 1983. [2](#)
- [MDDT] Gamal Mograby, Maxim Derevyagin, Gerald V. Dunne, and Alexander Teplyaev. Lax Pairs on graded graphs. (*In preparation*). [2](#)
- [MT95] Leonid Malozemov and Alexander Teplyaev. Pure point spectrum of the Laplacians on fractal graphs. *J. Funct. Anal.*, 129(2):390–405, 1995. [2](#), [12](#), [15](#), [18](#)
- [MT03] Leonid Malozemov and Alexander Teplyaev. Self-similarity, operators and dynamics. *Math. Phys. Anal. Geom.*, 6(3):201–218, 2003. [2](#), [18](#)
- [NT08] Volodymyr Nekrashevych and Alexander Teplyaev. Groups and analysis on fractals. In *Analysis on graphs and its applications*, volume 77 of *Proc. Sympos. Pure Math.*, pages 143–180. Amer. Math. Soc., Providence, RI, 2008. [2](#)
- [SKHR⁺03] Ferdinand Schmidt-Kaler, Hartmut Haefner, Mark Riebe, Stephan Gulde, Gavin Lancaster, Thomas Deuschle, Christoph Becher, Christian Roos, Jrgen Eschner, and R. Blatt. Realization of the cirac-zoller controlled-not quantum gate. *Nature*, 422:408–11, 04 2003. [1](#)
- [ST19] Benjamin Steinhurst and Alexander Teplyaev. Spectral analysis and dirichlet forms on Barlow-Evans fractals. *under revision, preprint arXiv:1204.5207*, 2019. [2](#), [8](#), [9](#)
- [Sze75] Gábor Szegő. *Orthogonal polynomials*. American Mathematical Society, Providence, R.I., fourth edition, 1975. American Mathematical Society, Colloquium Publications, Vol. XXIII. [11](#)
- [Tep08] Alexander Teplyaev. Harmonic coordinates on fractals with finitely ramified cell structure. *Canad. J. Math.*, 60(2):457–480, 2008. [2](#)
- [VZ12a] Luc Vinet and Alexei Zhedanov. How to construct spin chains with perfect state transfer. *Physical Review A*, 85(1):012323, 2012. [2](#)
- [VZ12b] Luc Vinet and Alexei Zhedanov. Para-Krawtchouk polynomials on a bi-lattice and a quantum spin chain with perfect state transfer. *J. Phys. A*, 45(26):265304, 11, 2012. [2](#)

APPENDIX A. HAMBLY-KUMAGAI DIAMOND GRAPHS: EIGENVALUES TABLE FOR LEVEL 3 & 4

Eigenvalues of \mathbf{H}_3 (Hambly-Kumagai diamond graph of level 3)

j	Eigenvalue λ_j	Multiplicity	j	Eigenvalue λ_j	Multiplicity
1	-4	1	9	1	1
2	$-\sqrt{\sqrt{46}+9}$	1	10	$\sqrt{9-\sqrt{46}}$	1
3	-3	1	11	2	1
4	$-2\sqrt{2}$	5	12	$2\sqrt{2}$	5
5	-2	1	13	3	1
6	$-\sqrt{9-\sqrt{46}}$	1	14	$\sqrt{\sqrt{46}+9}$	1
7	-1	1	15	4	1
8	0	22			

Eigenvalues of \mathbf{H}_4 (Hambly-Kumagai diamond graph of level 4)

j	λ_j	Multipl.	j	λ_j	Multipl.	j	λ_j	Multipl.	j	λ_j	Multipl.
1	-8.0	1	10	-4.242640	8	19	1.0	1	28	5.0	1
2	-7.999773	1	11	-4.0	1	20	1.321523	1	29	5.830951	8
3	-7.0	1	12	-3.806076	1	21	2.0	1	30	5.980884	1
4	-6.996920	5	13	-3.0	1	22	2.600793	5	31	6.0	1
5	-6.0	1	14	-2.600793	5	23	3.0	1	32	6.996920	5
6	-5.980884	1	15	-2.0	1	24	3.806076	1	33	7.0	1
7	-5.830951	8	16	-1.321523	1	25	4.0	1	34	7.999773	1
8	-5.0	1	17	-1.0	1	26	4.242640	8	35	8.0	1
9	-4.927369	5	18	0.0	86	27	4.927369	5			

APPENDIX B. LANG-PLAUT DIAMOND GRAPHS: EIGENVALUES TABLE FOR LEVEL 3

Eigenvalues of \mathbf{H}_3 (Lang-Plaut diamond graph of level 3)											
j	λ_j	Multipl.	j	λ_j	Multipl.	j	λ_j	Multipl.	j	λ_j	Multipl.
1	-32.0	1	28	-17.272791	1	54	0.0	44	80	17.272791	1
2	-31.999214	1	29	-17.0	1	55	1.0	1	81	18.0	1
4	-30.989328	1	30	-16.0	1	56	2.0	1	82	19.0	1
5	-30.0	1	31	-15.141636	2	57	3.0	1	83	19.721929	1
6	-29.936434	1	32	-15.0	1	58	3.047899	1	84	20.0	1
7	-29.086539	4	33	-14.656694	1	59	4.0	1	85	20.48943	2
8	-29.0	1	34	-14.0	1	60	5.0	1	86	21.0	1
9	-28.77233	1	35	-13.0	1	61	6.0	1	87	21.98050	1
10	-28.0	1	36	-12.020182	4	62	6.066367	1	88	22.0	1
11	-27.422949	1	37	-12.0	1	63	7.0	1	89	22.214599	4
12	-27.0	1	38	-11.89895	1	64	8.0	1	90	23.0	1
13	-26.0	1	39	-11.0	1	65	8.180098	2	91	24.0	1
14	-25.844467	1	40	-10.0	1	66	9.0	1	92	24.027192	1
15	-25.0	1	41	-9.026252	1	67	9.026252	1	93	25.0	1
16	-24.027192	1	42	-9.0	1	68	10.0	1	94	25.844467	1
17	-24.0	1	43	-8.180098	2	69	11.0	1	95	26.0	1
18	-23.0	1	44	-8.0	1	70	11.89895	1	96	27.0	1
19	-22.214599	4	45	-7.0	1	71	12.0	1	97	27.422949	1
20	-22.0	1	46	-6.066367	1	72	12.020182	4	98	28.0	1
21	-21.98050	1	47	-6.0	1	73	13.0	1	99	28.77233	1
22	-21.0	1	48	-5.0	1	74	14.0	1	100	29.0	1
23	-20.48943	2	49	-4.0	1	75	14.656694	1	101	29.086539	4
24	-20.0	1	50	-3.047899	1	76	15.0	1	102	29.936434	1
25	-19.721929	1	51	-3.0	1	77	15.141636	2	103	30.0	1
26	-19.0	1	52	-2.0	1	78	16.0	1	104	30.989328	1
27	-18.0	1	53	-1.0	1	79	17.0	1	105	31.0	1
									106	31.999214	1
									107	32.0	1

GAMAL MOGRABY, MATHEMATICS DEPARTMENT, UNIVERSITY OF CONNECTICUT, STORRS, CT 06269, USA

E-mail address: gamal.mograby@uconn.edu

MAXIM DEREVYAGIN, MATHEMATICS DEPARTMENT, UNIVERSITY OF CONNECTICUT, STORRS, CT 06269, USA

E-mail address: maksym.derevyagin@uconn.edu

GERALD V. DUNNE, MATHEMATICS & PHYSICS DEPARTMENT, UNIVERSITY OF CONNECTICUT, STORRS, CT 06269, USA

E-mail address: gerald.dunne@uconn.edu

ALEXANDER TEPLYAEV, MATHEMATICS & PHYSICS DEPARTMENT, UNIVERSITY OF CONNECTICUT, STORRS, CT 06269, USA

E-mail address: alexander.teplyaev@uconn.edu